EFFECT OF RTM DEFECTS ON MODE I & II DELAMINATION BEHAVIOUR OF 5HS WOVEN COMPOSITES

Adrian F Gill*, Paul Robinson*, Silvestre Pinho*, John Sargent*
***Imperial College London**

Keywords: *delamination, harness satin, woven, fibre volume fraction, resin transfer moulding*

Abstract

Composites produced by resin infusion techniques will inevitably suffer from variation in resin distribution due to imprecise fibre placement and distortion of the preform during mould closure and infusion. This paper describes an investigation into the effect of variations in fibre volume fraction (FVF) on mode I and mode II delamination behaviour for 5 harness satin (5HS) woven carbon-fibre/epoxy resin composites manufactured by resin transfer moulding (RTM). Additionally, the effect of satin face tow orientation on interlaminar toughness was investigated.

1 Introduction

Interlaminar fracture toughness is a measure of a material's resistance to delamination. Accurate measurement of fracture toughness is necessary due to the significance of delamination on the integrity of laminated composite structures. Furthermore, a clear understanding of the effect of fibre volume fraction (FVF) on a material's fracture toughness is important for composites produced by resin infusion techniques, which can suffer from variations in resin distribution.

Briscoe *et al* [1] investigated the effect of weave type, aerial weight and surface texture on G_{Ic} for aramid-fibre/epoxy composites. They found that although weave type has little effect, larger values of G_{Ic} were obtained for fabrics that contained higher densities of fibre-ends created by abrasion of the surface and for fabrics with coarser weaves. Additionally, G_{Ic} was found to increase significantly with increasing crack length, behaviour attributed to fibre bridging. It was proposed that fibre-ends migrating into the resin-rich interply region, as found on fabrics with high fibre-end densities and coarser weaves, were responsible for increasing fibre bridging. Alif *et al* [2] investigated the effect of weave structure and interface tow orientation on G_{Ic}. They found that while 'R' curves for plain weave were almost horizontal, indicating no change in fracture mechanism during crack propagation, twill and satin weaves had R curves which exhibited an initial increase. This was attributed to fibre bridging, although the extent of fibre bridging was limited by the interlacing of the weave and in all cases 'R' curves assumed a steady state plateau toughness. For the satin weaves higher toughness was observed for crack propagation between surfaces with the majority of tows oriented at 90^o to the crack direction than for predominately 0^o surfaces. This was attributed to transverse tow delamination in the 90^o surface pinning the crack and causing it to arrest, thereby increasing toughness. This did not occur in the 0^o surfaces due to the constraint imposed on the transverse tows by the interlaced longitudinal tows.

Bradley and Cohen [3] argued that the necessary resin plastic deformation zones for maximum resin toughness are constrained by the fibres and cannot fully develop, consequently limiting toughness. Thus, it was concluded that the optimal thickness of a resin interply region depends on the type of resin used. Ductile resins would yield maximum toughness with a thicker resin-rich zone, whereas for a brittle epoxy a very thin zone would be optimal. Russell [4] studied the influence of local interlaminar fibre distribution on fibre bridging for graphite-fibre/epoxy laminates and showed that the extent of fibre bridging is increased as the plies are brought together. Hunston *et al* [5] noted that the mode I fracture performance of a number of laminates made of nominally identical materials but manufactured by two different organisations (NASA and Hexcel) were consistently different. Samples manufactured by NASA were invariably 40%-100% tougher than those by Hexcel. This was because processes used by NASA resulted in significant 'fibre nesting' and intermingling between prepreg layers which did not occur with Hexcel fabricated laminates.

In summary, experimental evidence suggests that interlaminar fracture toughness is greatly influenced by FVF and weave surface texture. This current work will assess the effect of variation in FVF and interface tow orientation on the energy-absorbing processes that occur in mode I and II delamination of 5HS woven carbon-fibre/epoxy resin manufactured by resin transfer moulding.

Additionally, it is thought that there are no publications of the 4ENF applied to harness satin fabrics and only one for plain weave fabric [6]. The application of the 4ENF test to a 5 harness satin weave in this investigation achieves this.

The results of this investigation are likely to be applicable to other material systems and may lead to the design of woven fabrics with considerably improved interlaminar toughness.

2 Laminate Manufacture and Test Method

Harness satin weaves have ply asymmetry with one side predominately warp and the other predominately weft (Fig. 1). Careful design was required to create eight-ply lay-ups such that each arm and full laminate stayed flat after curing and the arms had equal flexural stiffness.

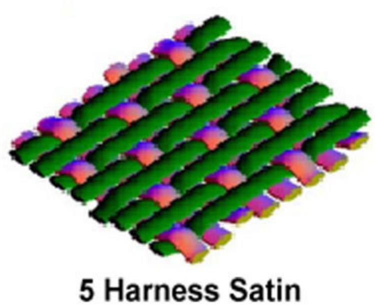

Fig. 1. 5 harness satin weave with ply asymmetry, from Ref (10).

Test panels with 0^o_{warp}-0^o_{warp} mid-plane satin face tow orientation were manufactured from 5HS woven carbon-fibre (G926, Tenax HTA 6K, 390g/m^2 including 3-6% E01 epoxy powder binder)/RTM6 epoxy resin using RTM with FVFs of 56.5%, 62.5% and 68.5%. Panels of 62.5% FVF were also manufactured with mid-plane satin face tow orientations of 0^o_{warp}-0^o_{warp} and 0^o_{warp}-90^o_{weft}. Mode I tests were performed using the double cantilever beam (DCB) [7] method and mode II using the 4-point end notched flexure (4ENF) [8].

3 Results

3.1 Mode I

In DCB tests, all four specimen types exhibited similar saw-toothed load-displacement behaviour (Fig. 2). This made it difficult to accurately determine critical energy release rate values from the curves. Fracture toughness can be calculated from the points associated with the onset of unstable crack growth (eg. point ‘A’ in Fig. 2) and for other points on the rising portion of the load-displacement curve associated with crack growth. However, the toughness between ‘A’ and ‘B’, the point where the crack arrests, must be lower than at ‘A’ (hence instability) indicating that the toughness at ‘A’ is a local maximum. Furthermore, the dynamics of the unstable crack growth mean that G_{Ic} calculated at ‘B’ is not necessarily a material toughness property. Thus, although G_{Ic} calculated from point ‘A’ is representative of the material fracture toughness and of use to the investigation, it must be noted that it is a local maximum.

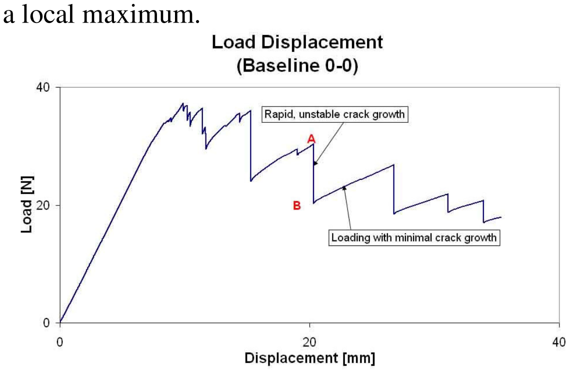

Fig. 2. Mode I baseline 0-0 (62.5% FVF) saw-toothed load-displacement behaviour.

Minimal variation in initiation toughness means between sample types was observed with considerable scatter within each sample type. This scatter in initiation toughness is thought to result from the location of the local toughness maxima relative to the starter film.

Inspection of G_{Ic} propagation values suggests that higher FVF and more transverse tows at the interface increases toughness. Tests of 0^o-0^o interface specimens with varying FVF indicate that the baseline FVF (62.5%) at 525 J/m^2 is 22% tougher than the low FVF (56.5%) at 430 J/m^2 and that the high FVF (68.5%) at 741 J/m^2 is 41% tougher than the baseline (Fig. 3). It was also observed that high FVF specimens can show considerable toughness rise with increasing crack length and that two types of ‘R’ curve behaviour types occurred, ‘rising’ and ‘flat’ (Fig. 4). Differences between the two high FVF behaviour types are also visible on recorded load-displacement traces. G_{Ic} propagation values from the 0^o-90^o

interface at 868 J/m^2 were over 60% tougher than the 0^o-0^o interface of the same FVF.

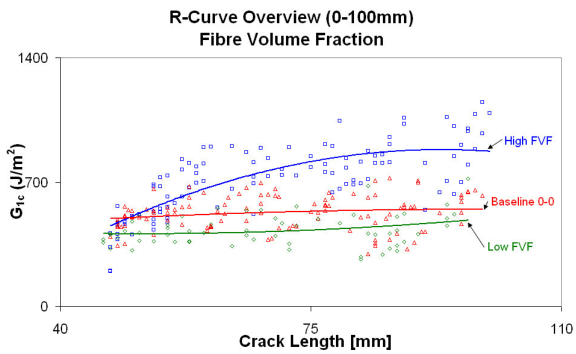

Fig. 3. Comparison of 'R' curves for varying FVF.

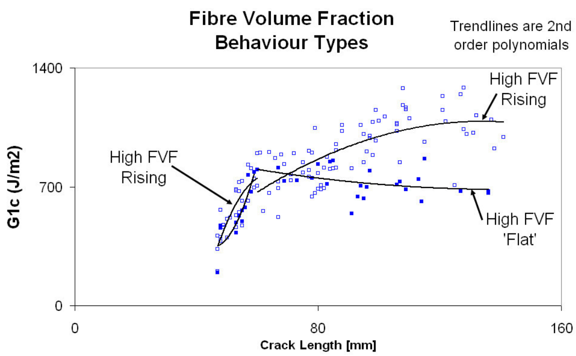

Fig. 4. High FVF R curves showing two distinct behaviour types.

Observations made during tests suggest that resistance to crack growth varies relative to the weave pattern and that the crack is arresting at transverse tows and growing unstably along longitudinal satin tows. Optical microsections (Fig. 5) taken within specimens away from the free edge confirm this and show transverse tow delamination and cracking, and suggest possible splitting of the longitudinal tows. This apparent longitudinal tow damage appears to initiate at transverse tow delaminations and may propagate considerable distances, increasing toughness. This contradicts the findings of Alif *et al* [2], who observed that the highly constrained transverse tows in the interior of the specimen did not debond during testing. To investigate this further, penetrant enhanced X-ray (Fig. 6) and C-scan images were taken. These indicate that a strong correlation exists between fracture sub-surface damage (including transverse tow delamination and cracking and longitudinal tow splitting) and the measured interlaminar fracture toughness (Fig. 3).

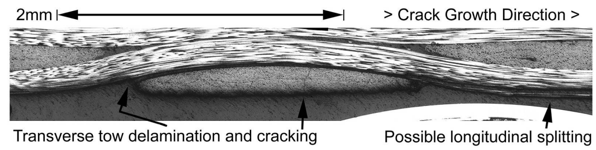

Fig. 5. Microsection from within a failed high FVF specimen showing damage.

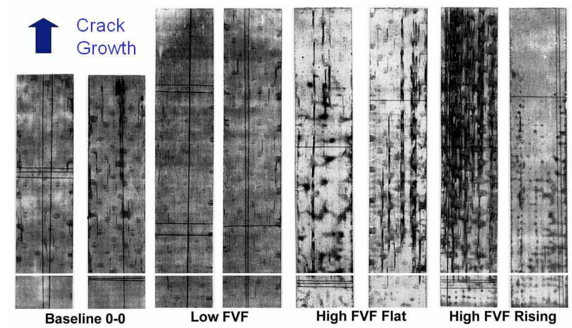

Fig. 6. X-rays of specimens with varying FVF show clear differences in sub-surface damage morphology that explains interlaminar toughness results.

3.2 Mode II

In 4ENF tests, significant damage including delamination and blistering as well as fibre fracture was found to occur in specimen arms (Fig. 7). This damage resulted in a drop in load and increase in compliance (Fig. 8). However, the linearity of the compliance curve suggests that damage only occurred at crack lengths in excess of 60mm and toughness values were therefore computed for crack lengths less than 60mm.

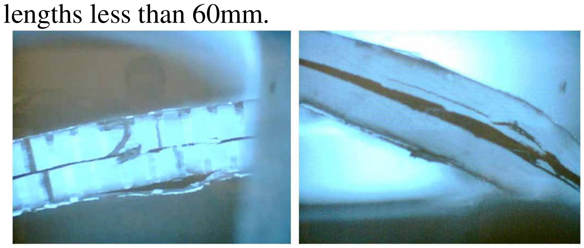

Fig. 7. Arm damage included delamination and blistering as well as in-plane fibre failure.

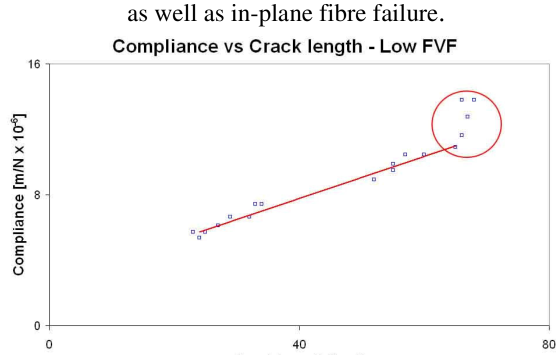

Fig. 8. Mode II compliance curve with arm damage highlighted.

Interlaminar toughness values of approximately 4000 J/m^2 were obtained for all FVFs in this way. These results are higher than anticipated and to investigate their validity, failed specimens were inspected for damage in the arms using microscopy and X-rays. Additionally, tests were repeated using specimens reinforced with bonded laminate strips to increase the arm stiffness and prevent bending failure occurring before interlaminar crack growth (Fig. 9). Reeder *et al* [11] have previously demonstrated that such reinforcements have no effect on 4ENF test data processing, although reinforcements of similar FVF to the specimens were used to mitigate Poisson's ratio effects from joining dissimilar materials.

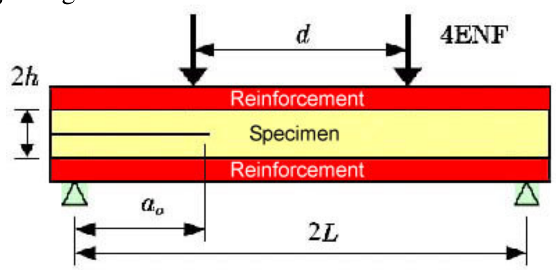

Fig. 9. Specimens were reinforced with bonded laminates of equal FVF.

Tests performed on reinforced specimens did not suffer bending failure in the arms and interlaminar toughness values of approximately 3000 J/m^2 were obtained. This is a significant reduction in measured toughness compared to the unreinforced specimens, suggesting that energy absorbing mechanisms are occurring in addition to mid-plane interlaminar cracking. This invalidates the unreinforced results.

However, a number of specimens with 68.5% FVF were found to debond from the reinforcements during testing raising questions about the validity of the reinforced specimen results. It is thought that additional energy absorption could be resulting from reinforcement debonding and work is being performed to assess whether this occurred in other reinforced specimens.

If debonding was found to occur, the reinforced specimens will be redesigned to minimise interlaminar shear at the reinforcement and further tests will be performed to evaluate G_{IIc}. As with mode I, post-processing techniques including micrography and X-ray will be used to investigate the relationship of surface morphology and subsurface damage to interlaminar toughness.

4. Conclusions

Interlaminar fracture toughness tests were performed in modes I and II to determine the effect of variation in fibre volume fraction on interlaminar toughness for a 5 harness satin woven fabric manufactured by RTM. Microscopy and X-ray imaging were performed on the specimens to determine the relationship of surface morphology and sub-surface damage to interlaminar toughness and important observations were made.

Acknowledgements

The support of Bristol University, Airbus, Shorts, Hexcel, ESPRC, DTI and MOD is gratefully acknowledged.

5. References

[1] Briscoe, B.J., Court, R.S. Williams, D.R. "The Effect of Fabric Weave and Surface Texture on the Interlaminar Fracture Toughness of Aramid/Epoxy Laminates" *Comp Sci Tech*, v47, pp261-270, 1993.

[2] Alif, N., Carlsson, L. A., Boogh, L., "The effect of weave pattern and crack propagation direction on mode I delamination resistance of woven glass and carbon composites", *Composites Part B, v*29, n5, pp603-611, 1998.

[3] Bradley, W. L., Cohen, R. N., *Delamination and Debonding of Materials, ASTM STP 876, pp*389-410, ASTM, 1985

[4] Russell, A. J., "Micromechanisms of interlaminar fracture and fatigue", *Polymer Composites,* v8, n5, pp342-351, 1987.

[5] Hunston, D.L., Moulton R. J., Johnston, N. J., Bascom, W. D., *Toughened Composites, ASTM STP 937, pp*74-94, ASTM, 1987.

[6] Paris, I., Minguet, P.J., O'Brien, K.T. "Comparison of delamination characterization for IM7/8552 composite woven and tape laminates", *ASTM Special Technical Publication,* n1436, pp 372-390, 2003.

[7] ASTM Standard D5528 – 94a, 1994.

[8] Martin R, Elms T, Bowron S. "Characterisation of mode II delamination using the 4ENF". *Proceeding of 4th European Conference on Composites: Testing and Standardisation*, Lisbon, Portugal, 1998.

[9] Hodgkinson, J. M., Robinson, P., *Mechanical Testing of Advanced Fibre Composites,* Woodhead, 2000

[10] Tang, X., Whitcomb, J.D., Li, Y., Sue, H.J., "Micromechanics modeling of moisture diffusion in woven composites", *Comp Sci Tech*, v65, n6, pp817-826, 2005.

[11] Reeder, J.R., Demarco, K., Whitley, K.S. "The use of doubler reinforcement in delamination toughness testing", *Composites. Part A*, v35, n11, pp1337-44, 2004.